Chapter 5

Electrocatalytic Reduction of CO_2 to Small Organic Molecule Fuels on Metal Catalysts

Wenzhen Li*

Department of Chemical Engineering, Michigan Technological University, Houghton, MI 49931, USA.
***Email: wzli@mtu.edu. Tel: 906-487-2298. Fax: 906-487-3213.**

The electrocatalytic reduction of carbon dioxide (CO_2) to liquid fuels has tremendous positive impacts on atomospheric carbon balance and help to reduce global warming issues. This paper reviewed current knowledge of electrochemical CO_2 reduction to small organic molecule fuels on metal catalysts and gas-phase CO_2 reduction techniques based on gas diffusion electrode and solid polymer electrolyte. Future research and development needs in this area were also discussed.

Keywords: carbon dioxide; electrocatytic reduction; synthetic fuels; electrochemistry; electro-driven conversion; catalysis; gas diffusion electrode; electrolysis; photoelectrochemical reactor

1. Introduction

The increase of carbon dioxide (CO_2) in the atmosphere is claimed to be one of the major contributors to the greenhouse effect and will result in serious global warming issues (*1–3*). The electrocatalytic reduction of CO_2 to liquid fuels is a critical goal that would positively impact the global carbon balance by recycling CO_2 into usable fuels (*4–8*). However, CO_2 is an extremely stable molecule generally produced by fossil fuel combustion and respiration, returning CO_2 to a useful chemical state on the same scale as its current production rates is beyond our current scientific and technology ability (*4*). No commercially available processes exist for the conversion of CO_2 to fuels and chemicals yet. The challenges presented are great, but the potential rewards are

In Advances in CO2 Conversion and Utilization; Hu, Y.;
ACS Symposium Series; American Chemical Society: Washington, DC, 2010.

enormous. To address this challenging scientific problem, we need to advance our fundamental understanding of the chemistry of CO_2 activation and develop novel multifunctional catalysts that could use electricity to efficiently break C-O bond and form C-H and C-C bonds (*4*). Appropriate energy input and reasonable productivity of fuels are also important considerations for practical industrial processes.

The CO_2 electrocatalytic reductions to usable fuels are 'reverse' electrochemical processes compared to the anode reactions occurred in fuel cells. CO_2 reduction converts electrical energy back to chemical energy stored in the chemical bonds of fuels. In thermodynamics, the Gibbs free energy of CO_2 reduction is always positive at medium and high pH range, and the theoretical potentials are negative. Thus, CO_2 reduction is an electrolysis process that requires electrical energy input. In kinetics, the overpotential needed to electrochemically reduce CO_2 is always > 1.0 V, to get reasonable amounts of fuels, such as methane, ethylene, etc. In an aqueous electrolyte, the water reduction always occurs, and H_2 is a major by-product accompanied with CO_2 reduction. High hydrogen overvoltage metals, such as Hg, can suppress H_2 evolution, but it leads to formation of formate ions ($HCOO^-$) at very high overpotentials (high energy cost).

A milestone work is that Hori group found the CO_2 reduction on copper (Cu) behaves very different from the other metals. Cu can directly reduce CO_2 to hydrocarbons (mainly methane and ethylene) with reasonable current density (i.e. 5-10 mA/cm^2) and current efficiency (i.e. > 69% at 0°C) in aqueous electrolyte (*6*, *9*). Cu-based catalysts (Cu single crystals, adatom Cu electrode, and Cu alloys electrodes) have been extensively studied from both fundamental and applied perspectives (*9–17*). Although the process has not been commercialized to produce hydrocarbon products yet, gas mixtures of hydrogen, methane, ethylene and CO would form 'hythane' that can be promoted as alternative fuel for existing vehicles (*18*).

CO_2 reduction in gas phase based on gas diffusion electrode (GDE) and solid polymer electrolyte (SPE) can greatly improve CO_2 transport, thus facilitating CO_2 reduction (*19–23*). Taking the advantages of established electrolysis cell and fuel cell technologies, electrocatalytic recycling of CO_2 and small organic molecule fuels appears to be a promising means to achieving sustainable, carbon neutral energy conversions. Recently, surprising long carbon chain organic molecules, such as iso-propanol and $C_{\geq 4}$ oxygenates, were found in the GDE based electrocatalytic reduction of CO_2 based on CNT-encapsulate metal catalysts (*24*, *25*), although in very small amounts, they might open new avenues to CO_2 electrocatalytic conversion to liquid fuels.

Some excellent review articles are already available in this field. Frese reviews CO_2 electrocatalytic reduction on solid electrodes (*5*), Gattrell focused on fundamental mechanisms of electrochemical reduction of CO_2 to hydrocarbons on copper electrode in aqueous electrolyte solution (*6*), and Hori recently gave a comprehensive review on CO_2 reduction on metal electrodes based on his pioneer work in this area (*7*). This paper will introduce current knowledge of electrochemical CO_2 reduction on heterogeneous metal catalysts, review present CO_2 reduction techniques based on GDE and SPE, and discuss future research and

In Advances in CO2 Conversion and Utilization; Hu, Y.;
ACS Symposium Series; American Chemical Society: Washington, DC, 2010.

development needs in this area. Although homogeneous catalysis is an efficient approach to CO_2 reduction (*8*), it is out of the scope of this paper.

2. Review

2.1. Fundamental Challenges for Electrochemical Reduction of CO_2

The products of CO_2 reduction vary from liquid fuels (i.e. formic acid and isopropanol), hydrocarbons (i.e. methane and ethylene) to fuel precursors (i.e. CO). The reactivity of CO_2 reduction is very low, however, the equilibrium potentials of CO_2 reduction are not very negative (equation 123456), compared to hydrogen evolution reaction (HER) in aqueous electrolyte solutions (equation 7). The primary reactions that occurred on electrode in aqueous solution at pH 7.0 at 25°C, versus standard hydrogen electrode (SHE) are shown below (*7*, *26*):

$$CO_2 + H_2O + 2e^- = HCOO^- + OH^- \quad (-0.43V) \quad (1)$$

$$CO_2 + H_2O + 2e^- = CO + 2OH^- \quad (-0.52\ V) \quad (2)$$

$$CO_2 + 6H_2O + 8e^- = CH_4 + 8OH^- \quad (-0.25\ V) \quad (3)$$

$$2CO_2 + 8H_2O + 12e^- = C_2H_4 + 12OH^- \quad (-0.34\ V) \quad (4)$$

$$2CO_2 + 9H_2O + 12e^- = C_2H_5OH + 12OH^- \quad (-0.33\ V) \quad (5)$$

$$3CO_2 + 13H_2O + 18e^- = C_3H_7OH + 18OH^- \quad (-0.32\ V) \quad (6)$$

$$2H_2O + 2e^- = 2OH^- + H_2 \quad (-0.41\ V) \quad (7)$$

CO_2 reduction does not occur easily and the real applied electrolysis potentials for CO_2 reduction are more negative than the equilibrium values. This is mainly because the single electron reduction of CO_2 to $CO_2^{\cdot-}$ (equation 8), which has been well recognized as the first step to activate CO_2 for subsequent reduction steps, occurs at -1.90 V, due to a large reorganizational energy between linear molecule and bent radical anion. This step has also been determined as the rate determining step (RDS) for CO_2 reduction.

$$CO_2 + e^- = CO_2^{\cdot-} \quad (-1.90\ V) \quad (8)$$

It should be noted that the theoretical equilibrium potentials decrease with pH increasing, governed by the Nernst equation (*6*). For example, the equilibrium

In Advances in CO2 Conversion and Utilization; Hu, Y.;
ACS Symposium Series; American Chemical Society: Washington, DC, 2010.

potential is +0.17 V for CO_2 reduction to methane at pH 0 (Equation 9). The equilibrium potentials over the range of pH values around where the reactions are typically carried out are shown in Fig. 1.

$$CO_2 + 8H^+ + 8e^- = CH_4 + 2H_2O \quad (+0.17V) \quad (9)$$

The key problem of the conversion of CO_2 to liquid fuels is the assembly of the nuclei and formation of chemical bonds to convert the relatively simple CO_2 molecule into more complex and energetic molecules. The CO_2 reduction is greatly limited by reaction kinetics. Considering their low equilibrium potentials as shown in Fig. 1, thermodynamically, the products of methane and ethylene should occur at a less cathodic potential than hydrogen, however, kinetically this does not happen.

The products distribution for CO_2 reduction on Cu electrode as a function of potential is plotted in Fig. 2. Initially, CO_2 reduction produces CO and formate until below -1.12V, where hydrocarbons begin to form, with first ethylene (C_2H_4), then methane (CH_4) appearing. The methane production shows the stronger potential dependence, and these reactions accelerate, dominating over CO and formate at around -1.35V. Therefore, the fundamental challenges for CO_2 reduction come from both thermodynamics and kinetics.

In addition, hydrogen evolution reaction (HER) takes place in aqueous electrolytes by cathodic polarization, competing with CO_2 reduction, HER is prevalent in acidic solutions, while CO_2 does not exist in a basic solution. Therefore, most CO_2 reduction study was conducted in close neutral electrolyte solutions (i.e. 0.05 – 0.5 M $NaHCO_3$).

2.2. Classification of Electrocatalytic Metals and Reaction Selectivity

The product selectivity in CO_2 reduction depends on many factors, such as concentration of the reactants, electrode potential, temperature, electrocatalyst material and electrolyte solution (i.e. aqueous or non-aqueous electrolyte). As widely accepted by most researchers, the electrocatalyst materials govern the selectivity of CO_2 reduction, when the other conditions are identical. Hori's group has carried out a series of elegant research on CO_2 reduction (*9–13*), and found electrocatalytic metals can be generally divided into four groups based on product selectivity, as shown in Table 1.

The 1st group metals include Pb, Hg, In, Sn, Cd, TI, Bi, etc. They have high hydrogen overvoltages, negligible CO adsorption properties, and high overvoltages for CO_2 to $CO_2^{\cdot-}$, and hence weak stabilization of $CO_2^{\cdot-}$. The major product is formate ion ($HCOO^-$).

The 2nd group metals include Au, Ag, Zn, etc. They have medium hydrogen overvoltages and weak CO adsorption properties, and the major product is carbon monoxide (CO). Because they can catalyze the breakage of the C-O bond in CO_2 but allow the CO desorb, thus, the major product is CO.

The 3rd group metals include Ni, Fe, Pt, Ti, etc. They have low hydrogen overvoltages and strong CO adsorption properties and the major product is H_2, because the main reaction is water reduction to H_2.

In Advances in CO2 Conversion and Utilization; Hu, Y.;
ACS Symposium Series; American Chemical Society: Washington, DC, 2010.

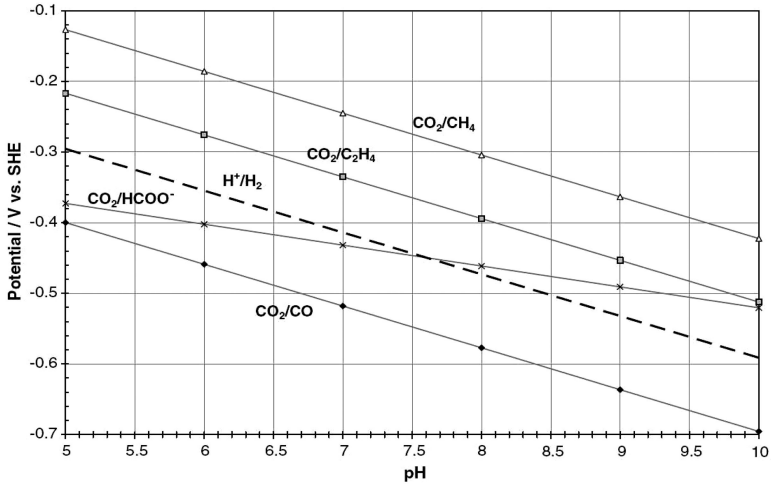

Figure 1. The equilibrium potentials as a function of pH for the principal CO_2 reduction reaction at 25°C (Ref. (7)). Copyright (2007) with permission from Elsevier.

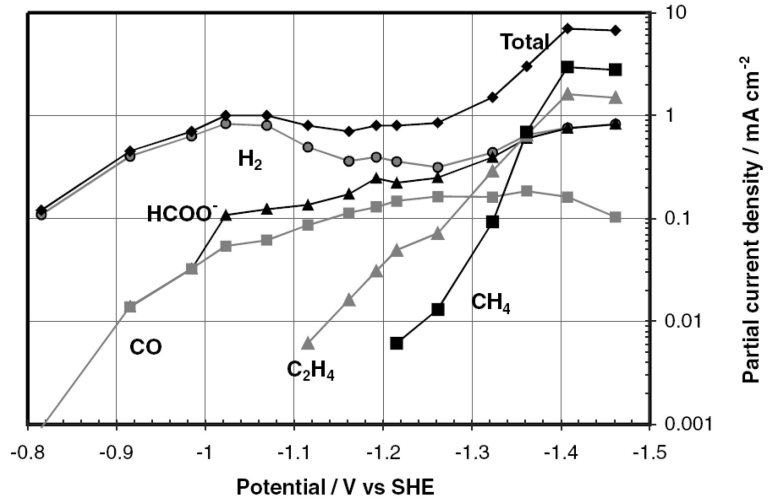

Figure 2. Partial current data obtained from high-purity Cu electrode from Ref (7), conditions: 0.1 M $KHCO_3$, 19°C, CO_2 bubbled, $[H^+]=1.55\times10^{-7}$ M, $[CO_2]=3.41\times10^{-2}$ M. Copyright (2007) with permission from Elsevier.

The 4th group: Cu. Cu is unique for CO_2 reduction, because it is able to further react CO to more reduced species, such as CH_4 and C_2H_4 with significant amounts. The detailed mechanisms are discussed in section 2.3.

Azuma et al. applied 32 metals to CO_2 reduction at similar conditions (-2.2 V vs. SCE, 0.05M $KHCO_3$) and confirmed these results given in Table 1 (from Hori's group). They showed that Cu is the unique metal that can reduce CO_2 to appreciable amounts of hydrocarbons CH_4 and C_2H_4, while Ni and Pt catalysts

scarcely give products in CO_2 reduction at ambient temperature and pressure, but can reduce CO_2 to CO or formic acid under elevated pressure (i.e. 60 atm). They also provided a classical roadmap for CO_2 electrocatalytic reduction on metal catalysts (*16*), which can be found in Ref (*16*).

It is interesting that the presence of small amount of foreign atoms on the electrode surface could greatly change the reaction selectivity of CO_2 reduction (*6*, *27*). These adatom modified electrodes were prepared by under potential deposition or overpotential deposition techniques. For example, at -1.44 V vs SHE, the CO selectivity of pure Cu is 69%, while that of Cd and Pd adatom modified Cu is 82% and 0, respectively.

2.3. Reaction Mechanisms

The CO_2 reduction on various metal electrodes has been extensively studied, but knowledge about CO2 reduction is still limited, the reaction mechanisms were mainly obtained base on observed charge transfer coefficients and reaction orders acquired from macroscopic electrochemical testing. The partially understood reaction mechanisms are discussed as follows.

a. Formation of $CO_2^{\cdot-}$ Is the Rate-Determining Step (RDS)

The CO_2 can be chemisorbed as a bent $CO_2^{\delta-}$ molecule, which is promoted by surface defects, alkali metal promoted surfaces, and possibly through X-rays or photoelectrons during measurements. The exact geometry of $CO_2^{\delta-}$ metal is unclear, and the possible structures for adsorbed $CO_2^{\delta-}$ are shown in Fig. 3. CO_2 is an 'amphoteric' molecule possessing both acid and basic properties. The adsorption and stabilization of $CO_2^{\delta-}$ are dominantly governed by the electrode metals. The electrode metals interact with carbon or oxygen or both in CO_2 to form carbon coordination or oxygen coordination, or mixed coordination adsorption mode, respectively. The $CO_2^{\delta-}$ species is most easily produced at surface defects or in the presence of sublyer coverage of an alkali metal. It is generally agreed that the formation of $CO_2^{\cdot-}$ is the rate-determining step at medium and high overpotential regions. Jordan and Smith firstly proposed the formation of $CO_2^{\cdot-}$ anion radical by one electron transfer to CO_2 is the initial step for subsequent reduction of CO_2, as shown in Fig. 4 (a) (*28*). Pacansky et al. studied scf ab initio molecular orbital energies and atomic population analysis of $CO_2^{\cdot-}$ at the minimum energy geometry and found the unpaired electron density at the highest occupied orbital is localized at C atom at 84% (*29*). This result suggests that $CO_2^{\cdot-}$ is ready to react as a nucleophilic reactant at the carbon atom. The standard potential of $CO_2^{\cdot-}$ formation is -1.90 V or -1.85 V vs SHE, -2.21 V vs. SCE in aqueous media (*30–32*). The transfer coefficient of RDS in the lower overvoltage region was found to be 0.67 (*33*). The $CO_2^{\cdot-}$ is mostly present freely in both aqueous and non-aqueous electrolyte solutions, and has been captured by ultraviolet spectroscopy (*34*).

Table 1. Faradaic efficiencies of products in CO_2 reduction at various metal electrodes. Electrolyte: 0.1 M $KHCO_3$ (T = 18.5 ± 0.5°C, Ref. (*12*)). Copyright (1995) with permission from Elsevier.

Electrode	Potential vs. SHE V	Current density mA cm^{-2}	Faradaic efficiency, %							
			CH_4	C_2H_4	EtOH[a]	PrOH[b]	CO	$HCOO^-$	H_2	Total
Pb	−1.63	5.0	0.0	0.0	0.0	0.0	0.0	97.4	5.0	102.4
Hg	−1.51	0.5	0.0	0.0	0.0	0.0	0.0	99.5	0.0	99.5
Tl	−1.60	5.0	0.0	0.0	0.0	0.0	0.0	95.1	6.2	101.3
In	−1.55	5.0	0.0	0.0	0.0	0.0	2.1	94.9	3.3	100.3
Sn	−1.48	5.0	0.0	0.0	0.0	0.0	7.1	88.4	4.6	100.1
Cd	−1.63	5.0	1.3	0.0	0.0	0.0	13.9	78.4	9.4	103.0
Bi[c]	−1.56	1.2	-	-	-	-	-	77	-	-
Au	−1.14	5.0	0.0	0.0	0.0	0.0	87.1	0.7	10.2	98.0
Ag	−1.37	5.0	0.0	0.0	0.0	0.0	81.5	0.8	12.4	94.6
Zn	−1.54	5.0	0.0	0.0	0.0	0.0	79.4	6.1	9.9	95.4
Pd	−1.20	5.0	2.9	0.0	0.0	0.0	28.3	2.8	26.2	60.2
Ga	−1.24	5.0	0.0	0.0	0.0	0.0	23.2	0.0	79.0	102.0
Cu	−1.44	5.0	33.3	25.5	5.7	3.0	1.3	9.4	20.5	103.5[d]
Ni	−1.48	5.0	1.8	0.1	0.0	0.0	0.0	1.4	88.9	92.4[e]
Fe	−0.91	5.0	0.0	0.0	0.0	0.0	0.0	0.0	94.8	94.8
Pt	−1.07	5.0	0.0	0.0	0.0	0.0	0.0	0.1	95.7	95.8
Ti	−1.60	5.0	0.0	0.0	0.0	0.0	tr.	0.0	99.7	99.7

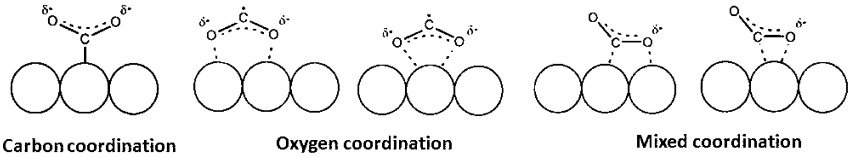

Figure 3. Possible structure for adsorbed $CO_2^{\delta-}$ on metals (Ref (7)). Copyright (2007) with permission from Elsevier.

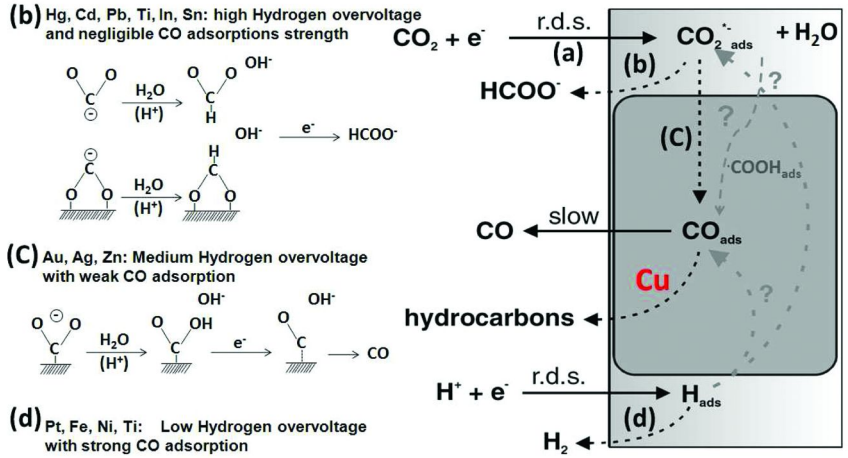

Figure 4. The main reaction pathways at the electrode surface, with adsorbed blocking the majority of the surface and hydrocarbon products being formed by the further reduction of adsorbed CO. (Ref (6, 7). Copyright (2007) with permission from Elsevier. (see color insert)

There are two main pathways for further reduction of adsorbed $CO_2^{\cdot-}$ to respective final product of CO, and formate ion ($HCOO^-$), which is governed by the properties of metal electrocatalysts.

b. Formation of Adsorbed $CO_2^{\cdot-}$ Leading to Further Reduction to $HCOO^-$

Erring et al. studied CO_2 reduction polarization data at Hg electrode in aqueous electrolyte with HCO_3^-, and obtained a major product of $HCOO^-$ (*35*). On Hg, CO_2 reduction is initiated by one electron transfer to form $CO_2^{\cdot-}$ at the potential negative of −1.6 V vs. SHE. The $CO_2^{\cdot-}$ will take a proton from a H_2O molecule at the nucleophilic carbon atom, forming $HCOO^{\cdot}$. H^+ will not be bonded to the O atom of $CO_2^{\cdot-}$, since p*K*a value of the acid-base couple ($CO_2^{\cdot-}/CO_2H$) is low of 1.4 (*36*). Hori et al found that the electrode potential is constant as the current density for $HCOO^-$ formation at a pH range of 2-8, thus, H_2O is believed to be the proton donor in the formate formation from $CO_2^{\cdot-}$. $HCOO^{\cdot}$ is subsequently reduced to $HCOO^-$ at the electrode in aqueous media. The reaction steps are:

In Advances in CO2 Conversion and Utilization; Hu, Y.;
ACS Symposium Series; American Chemical Society: Washington, DC, 2010.

$$CO_2^{\cdot -}{}_{ads} + H_2O \longrightarrow HCOO^{\cdot}{}_{ads} + OH^- \quad (10)$$

$$HCOO^{\cdot}{}_{\mathbf{ads}} + e^- \longrightarrow HCOO^- \quad (11)$$

Formate could also be produced directly by reaction with adsorbed hydrogen, which would be present as an intermediate in the hydrogen evolution reaction:

$$CO_2^{\cdot -}{}_{\mathbf{ads}} + H_{ads} \longrightarrow HCOO^- \quad (12)$$

Such a reaction mechanism would appear to be favored by $CO_2^{\cdot -}$ being adsorbed with oxygen coordination or being just close to the electrode. Other high hydrogen overvoltage electrodes, including Cd, Pb, Tl, In, and Sn, with weak adsorption of hydrogen, have high overvoltage for CO_2 reduction to $CO_2^{\cdot -}$, and hence weak stabilization of $CO_2^{\cdot -}$. The CO_2 reduction on these metals follows a similar mechanism as shown in Fig. 4 (b). In non-aqueous electrolyte, CO_2 electrolysis on Pb leads to formation of oxalic acid, due to formation of $(CO_2)_2^{\cdot -}$ (*6*).

c. Formation of Adsorbed $CO_2^{\cdot -}$ Leading to Further Reduction to CO

The other pathway also involves first protonation then reduction, which is similar to step b), however, the hydrogen appears to be added on oxygen not carbon in $CO_2^{\cdot -}$. The steps will occur more favorably on carbon coordination adsorption mode.

$$CO_2^{\cdot -}{}_{ads} + H_2O \longrightarrow {}^{\cdot}COOH_{ads} + OH^- \quad (13)$$

$${}^{\cdot}COOH_{ads} + e^- \longrightarrow CO_{ads} + OH^- \quad (14)$$

CO could be formed by a direct reaction with adsorbed hydrogen:

$$CO_2^{\cdot -}{}_{ads} + H_{ads} \longrightarrow CO_{ads} + OH^- \quad (15)$$

In these reactions, the electrophilic reagents, H_2O in aqueous solution, react with the O atom of adsorbed $CO_2^{\cdot -}$, forming CO_{ads} and OH^- as depicted in Fig. 4(c). Sasaki et al used an ab initio molecular orbital approach to study the configuration of $NiF(NH_3)_4(CO_2)$ as a model for CO_2 reduction and showed that C atom of CO_2 molecule is favorably coordinated with the transition metal atom in a complex and can be stabilized by a strong charge transfer due to back donation from Ni to CO_2, which indicates carbon coordination can facilitate protonation of oxygen (Eq.13), leading to formation of ${}^{\cdot}COOH$ not $HCOO^{\cdot}$.

At Au electrode, H^+ will not take part in the CO formation, since the partial current of CO formation is independent of pH. The CO_{ads} is readily desorbed from

In Advances in CO2 Conversion and Utilization; Hu, Y.;
ACS Symposium Series; American Chemical Society: Washington, DC, 2010.

the electrode as a gaseous molecule. The reaction scheme is suitable to other metal electrodes, such as Ag, Cu and Zn in aqueous media. The sequence of CO selectivity roughly agrees with that of the electrode potentials. This agreement verifies the hypothesis that CO is favorably produced from the electrode metals which stabilize $CO_2^{\bullet-}$ effectively. Because the CO adsorption on Au, Ag and Zn surface is weak, CO is the major product, as shown in Fig. 4 c. In comparasion, CO will be further reduced to hydrocarbon products on Cu electrode (as discussed in section 2.4).

d. Hydrogen Evolution Reaction (HER)

HER is a major side reaction that accompanies CO_2 reduction in an aqueous electrolyte. It has been found that the reaction kinetics of HER are pH dependent in the acid region and pH independent in the alkaline region. The HER can be written as

$$H^+ + e^- \longrightarrow H_{ads} \quad (16)$$

$$2H_{ads} \longrightarrow H_2 \quad (17)$$

$$\text{or} \quad H_{ads} + H^+ + e^- \longrightarrow H_2 \quad (18)$$

Adsorbed hydrogen H_{ads} and/or H^+ are the hydrogen source for hydrogenation in CO_2 reduction. Because CO is strongly adsorbed on Pt/Fe/Ni/Ti surface, in an applied potential range, the major product is H_2, rather than CO, as shown in Fig. 4 d.

2.4. Cu-Based Electrocatalysts

Cu is a unique metal that can reduce CO_2 to CH_4 and C_2H_4 and alcohols in aqueous electrolyte at low temperature (*6*). Some known mechanisms are reviewed as below.

a. Formation of CO_{ads} as Reaction Intermediate

From Fig. 2, at low overpotential, i.e. -0.9 V, the faradic yields of CO and $HCOO^-$ are both appreciable, while C_2H_4 begins to increase at -1.1V, CH_4 starts at -1.2V, these data indicate that CO and $HCOO^-$ may be precursors to hydrocarbons and alcohols. However, FTIR and Raman spectrum show CO is linearly adsorbed on Cu polycrystal electrode at -0.6V, which suggests that CO is the reaction intermediate formed at Cu electrode, serving as a precursor for further reduction to hydrocarbons and alcohols (*37*, *38*). The surface of the Cu electrode is covered by CO with coverage >90% as estimated from the current at -1.0V with and

without CO, this could severely suppress hydrogen evolution reaction. The heat of adsorption of CO on Cu is appropriate (-17.7 kcal/mol), which is higher than Au, but lower than Ni and Pt, as listed in Table 2 (*39*). Therefore, Cu allows efficiently subsequent reduction of CO to produce hydrocarbons and alcohols.

b. From CO_{ads} to Hydrocarbons

Since CO has been identified as a primary reaction intermediate for formation of hydrocarbons, CO was used to investigate mechanisms of CO_2 reduction on Cu. Fig. 2 suggests that CH_4 formation starts at a more negative potential than C_2H_4 (-1.22 vs -1.12 V), but C_2H_4 formation is more favorable in high pH media. In addition, the Tafel slope for the two reactions are very different. All these strongly indicate that formation of CH_4 and C_2H_4 is through different reaction pathways from common starting substance CO. Interestingly, the evidence of lack of formation of methanol implies that the C-O bond of CO is broken early and consistently in the mechanism.

For the case of formation of CH_4, the transfer efficient of > 1 suggests that there is an initial electron transfer in equilibrium before RDS, this could result in a CO anion radical, as shown in Fig. 5 (a). Ab initio calculations were used to evaluate the state of the adsorbed CO anion radical, a slight decrease of the Cu-C bond and an increase of the C-O bond to about 1.25 Å were found, this predicts a mostly double bond character (*40*).

There are two possible reaction paths after formation of CO anion radicals. The first path is shown in Fig. 5 (b). This path involves a proton in the reaction, which must occur reversibly before the second electron transfer for RDS to yield the observed transfer coefficient. This is an acid-base reaction at the oxygen. The formation of four C-H bond would be not reversible, leading to production of CH_4. The second path involves reaction of C-O anion radical with an adsorbed hydrogen. Once the adsorbed CO has been electrochemically split, the hydrogen will add on carbon to form C-H radical and result in formation of CH_4, as shown in Fig. 5(c).

For the case of C_2H_4 formation, ethylene formation begins at a lower potential without a pH dependence and with first electron transfer as the RDS. As the first electron transfer begins a reaction pathway that subsequently results in a two carbon product, it is reasonable to assume that some type of bond formation occurs in this reaction step. A reaction is proposed that involves a "prior association" of two adsorbed CO (see Fig. 6). The postulation of a starting "associated pair" of adsorbed CO also would be consistent with the lower activation potential vs. the formation of CO (and hence methane).

The other possible reaction path is through the step of $–CH_2$ (ads) with CO. Since C(ads) is readily reduce to $–CH_2$ as shown in Fig. 5 b, two $–CH_2$ can dimerize to form C_2H_4, or alternatively, CO inserts into $–CH_2$ to form $–COCH_2$ which is further reduced to C_2H_4, as shown in Fig. 6.

So far, we still lack convinced experimental data i.e. FT-IR / Raman spectrum under real reaction conditions, to clearly elucidate the elementary steps for the complex CO_2 reduction to hydrocarbons. It is still not very clear how H species

In Advances in CO2 Conversion and Utilization; Hu, Y.;
ACS Symposium Series; American Chemical Society: Washington, DC, 2010.

Table 2. CO reduction in 0.1 M $KHCO_3$ at various metal electrodes (Ref (*11*)). Copyright (1987) with permission from Japan Chemical Society.

Electrode	Potential V vs.SHE	Faradaic efficiency/ %				CO heat of adsorption kcal mol^{-1} [c]
		CH_4	C_2H_4	Other HCs and alcohols[b]	H_2	
Au	–1.49	0.0	0.0	0.0	101.6	9.2
Cu	–1.40	16.3	21.2	12.5	45.5	17.7
Ni	–1.46	2.6	0.3	0.7	94.2	40.8
Pt	–1.29	0.1	0.0	0.0	96.8	46.6

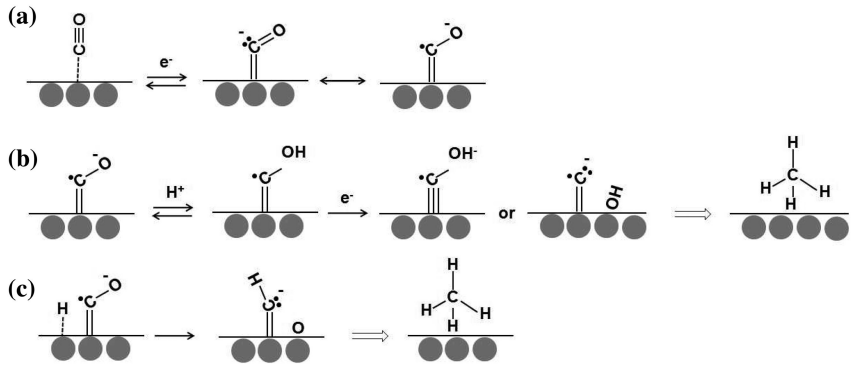

Figure 5. (a) the expected mechanism for initial electron transfer to adsorbed CO, (b) (c) the reaction mechanisms that could lead to the observed transfer coefficient and reaction order with pH. Grey particle: Cu atom, (Redrawn based on Ref (7)). Copyright (2007) with permission from Elsevier.

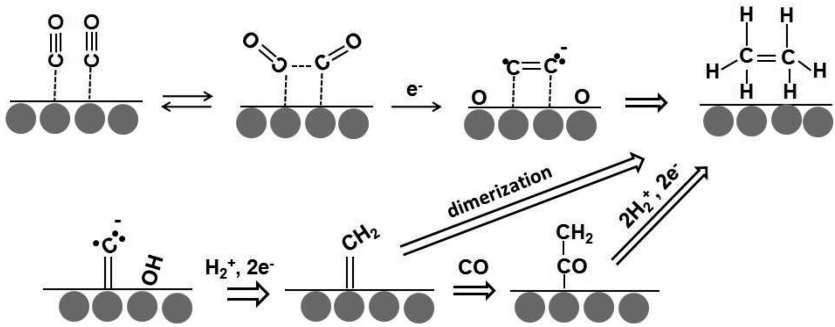

Figure 6. The proposed reaction mechanisms for producing a two carbon product. Grey particle: Cu atom, (Redrawn based on Refs. (6, 7)). Copyright (2007) with permission from Elsevier.

react with $CO_2^{\cdot-}$ or CO to generate hydrocarbons on Cu electrodes, the detailed reaction steps are question marks, as shown in Fig. 4.

In Advances in CO2 Conversion and Utilization; Hu, Y.;
ACS Symposium Series; American Chemical Society: Washington, DC, 2010.

The crystal faces dominated by Cu(100) tend to result in a significant current efficiency for ethylene at relatively low overpotentials (*41*), one possible reason might be related to the hypothesized rate determining step in Fig. 7. Such step would require the π orbitals of the adsorbed CO to interact simultaneously with vibrational motions bringing the two oxygens close to Cu surface atoms. Such an intermediate state would be more likely with a right arrangement of surface atoms, preferably with wide Cu (100) terrace surfaces (see Fig. 7, ref (*7*, *41*)).

The crystal faces dominated by Cu(111) tend to be polarised to more negative potentials and favor methane production. The Cu(110) type surfaces polarise to the most negative potentials and result in other 2 carbon and 3 carbon product, such as acetic acid (*42*). The product partial currents for methane and ethylene at polycrystalline Cu, Cu(100), Cu(110) and Cu(111) electrodes generally followed the same trends (*7*).

The overall CO_2 reduction required a higher overpotential, and a greater difference in overpotentials was found between the different crystal faces. The results of single crystal studies show why the electrode preparation could have a strong influence on the results obtained. Metallic nanostructures will be expected to provide more opportunities in deliberately produce more advantageous crystalline (*43*, *44*), i.e. nanocube is rich in (100), thus, improving the productivity of long-carbon chain organic molecules from CO_2 reduction. In addition, it was found that no simple choice of rate determining steps from among reactions fit the data, it implies that shifting and/or parallel mechanisms operate, varying electrode preparation and possibly electrolyte compositions might change the mechanisms.

c. Surface Treatment and Cu Alloy Electrocatalysts

Surface treatments affect the activity and selectivity of CO_2 reduction on Cu catalysts (*45–47*). Formation of CH_3OH was reported at intentionally preoxidized Cu electrodes, and the maximum partial current of CH_3OH production reached 15 mA/cm^2 (*48*). However, other researchers did not detect CH_3OH from Cu electrodes oxidized in various manners (*46*). Steady formation of CH_3OH from Cu electrodes at a high current density has not yet been confirmed by other researchers to date (*6*).

Cu-based alloys have been investigated for CO_2 reduction. The modifications can be due to a combination of changes in the electronic structure and changes in the surface crystallographic characteristics, including the introduction of dislocations and vacancies, leading to major changes in the products distributions and reaction rates. Cu-Ni and Cu-Fe alloys, formed by in-situ deposition during CO_2 reduction, gradually lose CH_4 and C_2H_4 yields simultaneously with increased H_2 evolution with the increase of Ni or Fe coverage on the Cu surface (*49*). A Cu-Cd electrode produced CH_4 and C_2H_4. The yields gradually dropped with the increase of Cd coverage, but the CO formation increased (*47*). Watanabe et al. studied various Cu based alloys; Cu-Ni, Cu-Sn, Cu-Pb, Cu-Zn, Cu-Cd, and found that the major products are CO and $HCOO^-$. Surface Cu-Au alloy electrodes showed that the surface alloying severely suppresses the formation of hydrocarbons and alcohols, leading to the increase of CO formation (*14*).

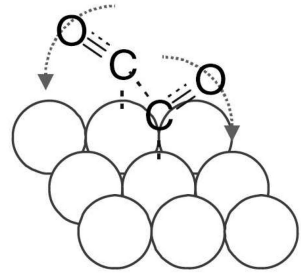

Figure 7. One possible mechanism for the catalysis of C_2H_4 formation on Cu (100) crystal (Ref. (7)). Copyright (2007) with permission from Elsevier.

2.5. Major Issues Associated with Aqueous CO_2 Reduction

Numerous researches have been carried out to investigate electrocatalytic reduction of CO_2 in aqueous phase and advanced the understanding of the reaction mechanisms. However, liquid phase CO_2 electrocatalytic reduction suffers from serious problems which are difficult to overcome:

1) Sluggish reaction kinetics: this leads to >1.0 V overpotential, which greatly increases the energy cost for electrolysis process.
2) Low selectivity of CO_2 reduction. CO_2 reduction and hydrogen evolution are two competitive reactions, hydrogen is inevitably a by-product accompanying with CO_2 reduction in aqueous electrolyte.
3) Formation of various by-products: they mainly remain in electrolyte solution and separation and recovery are high energy-cost.
4) Low solubility of CO_2 in aqueous electrolyte (≈ 0.08M): high pressures are normally needed to improve CO_2 transport.
5) Deactivation: the electrode catalysts loose their high initial selectivity and reactivity after a short period of operation.
6) Low tolerance to impurities and contaminations: The surface contamination and non-pure electrolyte will often lead to low productivity and selectivity of hydrocarbon products.

2.6. Gas Phase CO_2 Reduction Based on Gas Diffusion Electrode (GDE) and Solid Polymer Electrolyte (SPE)

An excellent alternative to CO_2 reduction in aqueous electrolyte is the use of GDEs and SPE (including cation exchange membrane (CEM) and anion exchange membrane (AEM)) for a continuous CO_2 reduction system which could enable considerable enhancements of mass transfer of CO_2 (*19–23*, *49–69*). GDE is a porous composite electrode developed for fuel cell technology, usually composed of Teflon bonded catalyst particles and carbon black. SPE membrane with GDE can provide gas phase electrolysis of CO_2. The acquired knowledge for CO_2 reduction over metal electrodes in aqueous electrolyte has been used to investigate the GDE/SPE-based electrolysis cells to convert CO_2 into usable fuels or syngas

In Advances in CO2 Conversion and Utilization; Hu, Y.;
ACS Symposium Series; American Chemical Society: Washington, DC, 2010.

H_2/CO, with reasonably good energy efficiencies. The main advances in this area are summarized as follow.

a. From CO_2 to Fuel Precursors (CO and H_2)

It is relatively easy to electrocatalytic reduce CO_2 to CO using the 2nd group metals (Table 1), such as Au, Ag, etc, or to reduce H_2O to H_2 (HER) using the 3rd group metals (Table 1), such as Ni, etc.

Yamamoto et al conducted CO_2 reduction and water oxidation in a CO_2-reducing electrolysis cell with Ni catalyst, 1/1 CO/H_2 gas ratio at a current density of 10 mA/cm^2 at a cell voltage of 3.05V was obtained, the overall energy efficiency is 44.6% (*49*).

Newman group has demonstrated a method for CO_2 and water reduction for making syngas (CO+H_2) operated at room temperature by employing GDEs embedded with an aqueous $KHCO_3$ (pH buffer) layer between the Au/Ag based cathode catalyst layer and the Nafion membrane (*4*, *55*). The schematic representation of the electrolysis cell is shown in Fig. 8. The cathode catalyst is Au or Ag, and the gas products are CO and H_2. Each catalyst was shown very selective for CO_2 reduction to CO at an overall current density of 20 mA/cm^2 for Ag and Au, respectively with the balance corresponding to H_2. A lower overpotential of 200 mV was observed on Au catalyst than Ag catalyst. As the overall current density efficiency increases, a decrease in CO current efficiency was observed, likely related to CO mass-transport limitation. Energy efficiency for the overall cell (with Pt-Ir as anode catalyst) is ca. 47% at 20 mA/cm^2 and decrease to ca. 32% at 100 mA/cm^2 for both catalysts, which is mostly due to joule heating losses. Their recent investigation show the CO partial current densities as high as 135 mA/cm^2 could be obtained for a short period based on supported Au catalyst (*4*). A CO/H_2 ratio of 1/2 was obtained, especially suitable for methanol synthesis, at a potential of ca. -0.2V vs SCE with a total current density of 80 mA/cm^2. Unfortunately, a decrease of catalyst selectivity for CO evolution with time has been identified as a critical technical issue (*55*).

b. From CO_2 to C_1-C_2 Fuels (Formic Acid, Methane and Ethylene)

An alternative possibility is to convert CO_2 to formic acid, that can be used as both fuels and chemicals. The 'Formic Acid Economy' was advocated by the UK government to promote sustainable energy development. Mahmood et al. demonstrated high rates of reduction of CO_2 to formic acid at Pb impregnated GDEs operated at 115 mA/cm^2 in aqueous acidic electrolytes (pH of 2) with a current efficiency of nearly 100% at an IR-corrected potential of 1.8 V (vs SCE) (*19*). Furuya et al. showed a current efficiency of 90% for the formation of formic acid at a GDE impregnated with Ru–Pd catalysts that can be obtained at the current density of 80 mAcm^2 (*22*).

The research efforts on CO_2 reduction to $C_{\leq 2}$ hydrocarbons (mainly methane and ethylene) using SPE cells were also studied. Hara et al. observed high

In Advances in CO2 Conversion and Utilization; Hu, Y.;
ACS Symposium Series; American Chemical Society: Washington, DC, 2010.

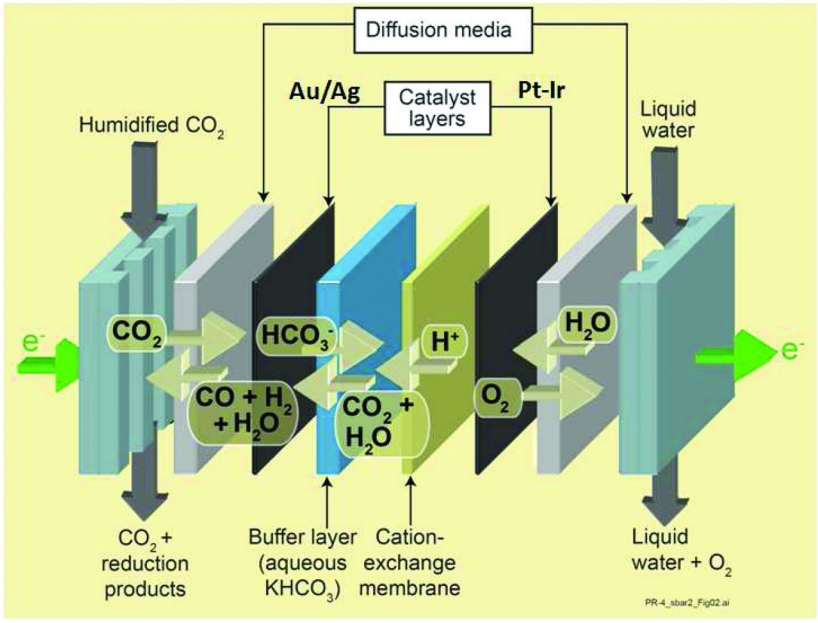

Figure 8. Schematic representation of an electrolysis cell for producing synthesis gas (CO + H_2) by reduction of CO_2 and H_2O. (Ref. (4)). (see color insert)

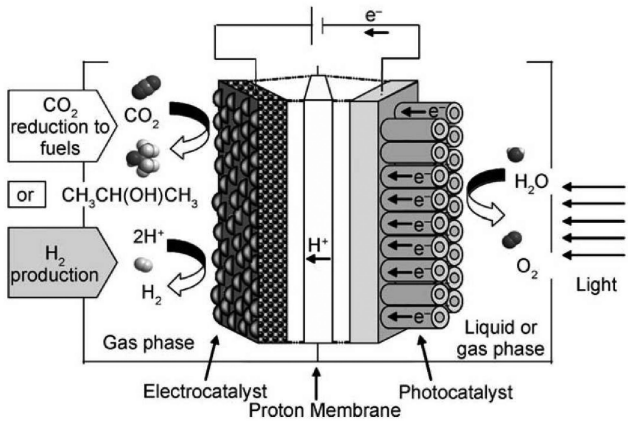

Figure 9. A proposed photoelectrochemical (PEC) device for the CO_2 reduction to fuels and the H_2 production using solar energy. (Ref (70)) Copyright (2010) with permission from Wieley.

current density attainment up to 900 mA/cm_2 and 46% faradaic efficiency during the reduction of CO_2 with the formation of methane on the GDE using Pt electrocatalysts at increased CO_2 pressures of 50 atm (*21*). DeWulf et al. applied an SPE with Cu as the catalyst layer on a Nafion 115. CH_4 and C_2H_4 were produced, but the current density for CO_2 reduction dropped below 1 mA/cm^2 after 70 min electrolysis, which indicates a durability issue (*56*). Sammells et al.

prepared a Cu coated SPE electrode using a CEM Nafion 117, and they found CO_2 was reduced to C_2H_4 and C_2H_6 with the current density of 10 to 30 mA/cm^2 with the terminal voltage 1.5 to 3.5 V. The faradaic efficiency for CO_2 reduction remained < 10% (*57–59*). Kamatsu et al studied Cu deposited on cation exchange membrane (CEM, Nafion) and anion exchange membrane (AEM, Selemion) and found the total efficicencies for CO_2 reduction has maximum values of 19% and 27%, respectively. The use of CEM gave C_2H_4 as the major product, while, with use of AEM, the HCOOH and CO were obtained. It is also interesting to find that NO has no influence on the CO_2 reduction, but the removal of SO_2 is needed to obtain C_2H_4 on high current densities (*61*). The best results in term of hydrocarbon formation were reported using immobilized CuCl on Cu mesh electrodes, a Faradic efficiency of about 70% for ethylene was obtained, even if the presence of a fast deactivation (*60*).

c. From CO_2 to Long-Chain Carbon Fuels

An ultimate goal for CO_2 cycling is direct reduction of CO_2 to liquid long-chain carbon fuels. It is still very challenging to achieve direct reduction CO_2 to such fuels based on current science and technology ability. Both the selectivity and productivity are very low and they are far from real applications.

It was reported that very small amount of parraffins and olefins up to C_6 hydrocarbons can be obtained in CO_2 electroreduction at room temperature and atmospheric pressure through commercially available Cu-electrode. Certain Cu-electrodes produce products in CO_2 electroreduction with a distribution as typically obtained in the Fischer–Tropsch reaction of syn-gas over heterogeneous Co- or Fe-based catalysts. The paraffin products fit to Schultz-Flory product distribution with an exception of olefins C_2H_4, which suggests that C_2H_4 is produced via another reaction path than chain propagation (*70*).

A new concept of photoelectrocatalytic (PEC) reactor was proposed in Fig. 9. At the anode, the water is photooxidized to oxygen and produce electrons and protons, which electrocatalytic reduce CO_2 to liquid fuels at the cathode (*71*). This concept was originally proposed by Hitachi Green Center researchers (*72*, *73*). Centi group reported Fe and Pt nanoparticles / carbon nanotubes (CNTs) exhibit encouraging electrocatalytic selectivity to CO reduction, the isopropanol can be the major product at a formation rate of 0.06 $\mu mol.h^{-1}.cm^{-2}$, besides CO and H_2 (Fig. 10 a). Other long carbon-chain hydrocarbons were detected in trace amounts.

It has been reported that the selectivity of CO_2 reduction to $C_{<2}$ hydrocarbons with the micropores of activated carbon fibers could be significantly enhanced, due to a special nanospace effect, which gives rise to a similar high-pressure-like effect at ambient pressure (*52*). As a unique support material, CNTs-based catalysts have demonstrated high activity and superior durability in low temperature fuel cell applications (*76–79*). The Bao group recently revealed that CNTs channels could provide an intriguing confinement environmental for Fisher-Tropsch synthesis (*80*, *81*). The strategy of design and preparation of catalysts could be widely applied to other gas-liquid reaction systems, such as CO_2 reduction to liquid fuels. As what Centi group demonstrated in their recent publications, the CNTs encapsulated Fe

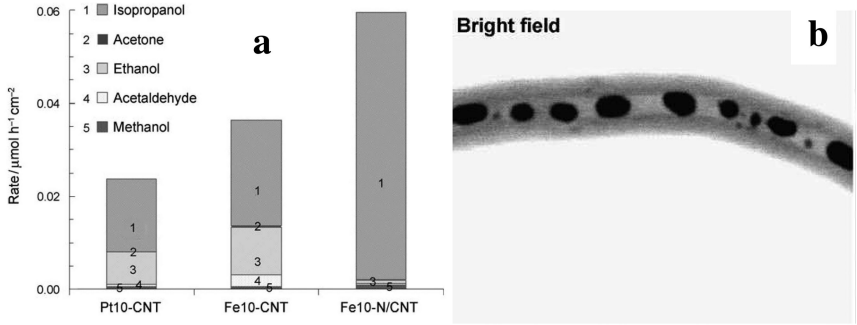

Figure 10. (a) Products distribution at 60°C in CO_2 reduction in gas phase over Nafion 117 cation exchange membrane /carbon cloth GDM electrode, (b) Fe encapsulated in CNTs. (Ref (24)) Copyright (2009) with permission from Elsevier.

nanoparticles (Fig. 10 b) can effectively promote long-carbon chain oxygenates, due to 'space-restriction' effect (*24*, *25*, *74*, *75*).

3. Conclusions and Future Directions

CO_2 is an extremely stable molecule generally produced by fossil fuel combustion and respiration, electrocatalytic approaches have potentials to direct convert CO_2 to small carbon chain fuels. The energy-efficient CO_2 reduction demand catalysts that can operate near thermodynamic potentials with high rate of electrochemical reaction. However, our current understanding on the reaction mechanisms is still very limited, and controllably returning CO_2 to useful carbon-fuels on the same scale as their current production rates is beyond our current scientific and technology ability. Conversion of CO_2 to liquid fuels and useful chemicals will require new methods and approaches for activating the CO_2 molecule. Novel complex catalysts and catalyst assemblies including hybrid catalysts, hierarchal nanostructured catalytic systems, and multi-site catalysts, that can work in concert, should be studied to achieve the overall efficient CO_2 reduction process.

It is imperative to advance our understanding of the reaction mechanisms of C-O bond cleavage and C-C and C-H bonds formation (especially for >2 carbon-chain molecules). Multi-step, multi-electron chemical transformations, coupled charge and atom transfer reactions are needed to be thoroughly investigated. At the mean time, developing advanced *in-situ* / *on-site* characterization tools under 'real' electrochemical operations is demanded to identify the key reaction intermediates and elucidate reaction pathways. The 'space-restriction effects' were discovered to change the reaction pathways, investigations on the interplay between various catalytic sites and catalyst environments in multifunctional catalysts are required. Extensive study on the model catalysts, including single crystal, atatom, and electro-deposited catalysts for CO_2 reduction have been carried out, bridging the gap between model catalysts and '*real-word'* nanostructured catalysts is highly demanded. Nano-techniques

provide exciting opportunities in this area by precisely controlling the surface facets, morphologies and structures of multi-metal nanoparticles.

In the future, research efforts should also be focused on addressing the engineering issues related with design and construction of electrolysis cells and photoelectrocatalytic reactors, fabrication of electrodes, assembly of membrane electrode and solid electrolyte, etc. The efforts will help realize efficient CO_2 recycling processes and devices.

Acknowledgments

I acknowledge fruitful discussions with Drs. Overbury, Steve and Wu, Zili of Oak Ridge National Laboratory (ORNL). I also thank Michigan Technological University start-up fund (D90925) and research excellence fund – research seeds (RES-RS, E49236) for supporting this work.

References

1. Halmann, M. M.; Steinberg, M. *Green Gas CO_2 Mitigation*; CRC Press: Boca Raton, FL, 1999.
2. Socolow, R.; Pacala, S. *Science* **2004**, *305*, 968.
3. Song, C. S. *Catal. Today* **2006**, *115*, 2.
4. Bell, A. T. Basic Research Needs: Catalysis for Energy; Report from the U.S. Department of Energy, Basic Energy Sciences Workshop; 2007, p 69.
5. Frese, K. W., Jr. In *Electrochemical and Electrocatalytic Reactions of Carbon Dioxide*; Sullivan, B. P., Krist, K., Guard, H. E., Eds.; Elsevier: Amsterdam, 1993; p 145.
6. Hori, Y. Electrochemical CO_2 Reduction on Metal Electrodes. In *Modern Aspects of Electrochemistry*; Springer: New York, 2008; pp 89−189.
7. Gattrell, M.; Gupta, N.; Co, A. *J. Electroanal. Chem.* **2006**, *594*, 1.
8. Benson, E. E.; Kubiak, C. P.; Sathrum, A. J.; Smieja, J. M. *Chem. Soc. Rev.* **2009**, *38*, 89–99.
9. Hori, Y.; Kikuchi, K.; Suzuki, S. *Chem. Lett.* **1985**, 1695.
10. Hori, Y.; Kikuchi, K.; Murata, A.; Suzuki, S. *Chem. Lett.* **1986**, 897.
11. Hori, Y.; Murata, A.; Takahashi, R.; Suzuki, S. *Chem. Lett.* **1987**, 1665.
12. Hori, Y.; Wakebe, H.; Tsukamoto, T.; Koga, O. *Electrochim. Acta* **1994**, *39*, 1833.
13. Hori, Y.; Takahashi, R.; Koga, O.; Hoshi, N. *J. Phys. Chem. B.* **2002**, *106*, 15.
14. Watanabe, M.; Shibata, M.; Kato, Azuma, M.; Sakata, T. *J. Electrochem. Soc.* **1991**, *138*, 3382.
15. Katoh, A.; Uchida, H.; Shibata, M.; Watanabe, M. *J. Electrochem. Soc.* **1991**, *141*, 2054.
16. Azuma, M.; Hashimoto, K.; Hiramoto, M.; Watanabe, M.; Sakata *J. Electrochem. Soc.* **1990**, *137*, 1772.
17. Cook, R.; MacDuff, R. C.; Sammells, A. F. *J. Electrochem. Soc.* **1988**, 1320.
18. Lynch, F. E.; Marmaro, R. W. U.S. Patent 5,139,002, 1992.

19. Mahood, M. N.; Masheder, D.; Harty, C. J. *J. Appl. Electrochem.* **1987**, *17*, 1159.
20. Hara, K.; Kudo, A.; Sakata *J. Electroanal. Chem.* **1995**, *391*, 141.
21. Hara, K.; Kudo, A.; Sakata; Watanabe, M. *J. Electroanal. Chem.* **1995**, *342*, L57.
22. Furuya, N.; Yamazaki, T.; Shibata, M. *J. Electroanal. Chem.* **1997**, *431*, 39.
23. Lee, J.; Kwon, Y.; Machunda, R. L.; Lee, H. J. *Chem.-- Asian J.* **2009**, *4*, 1516.
24. Gangeri, M.; Perathoner, S.; Caudo, S.; Centi, G.; Amadou, J.; Begin, D.; Pham-Huu, C.; Ledoux, M. J.; Tessonnier, J. P.; Su, D. S.; Schlogl, R. *Catal. Today* **2009**, *143*, 57.
25. Venti, G.; Perathoner, S.; Wine, G.; Gangeri, M. *Green Chem.* **2007**, *9*, 671.
26. Dean, A. J. *Lange's Handbook of Chemistry*, 13th ed.; McGraw-Hill: New York, 1985; Vol. 6-2, pp 9-4−9-107.
27. Hori, Y.; Wakebe, T.; Tsukamoto, T.; Koga, O. *Electrochim. Acta* **1994**, *39*, 1833.
28. Jordan, J.; Smith, P. T. *Proc. Chem. Soc.* **1960**, 246.
29. Pacansky, J.; Wahlgren, U.; Bagus, P. S. *J. Chem. Phys.* **1975**, *62*, 2740.
30. Lamy, E.; Nadjo, L.; Savéant, J.-M. *J. Electroanal. Chem.* **1977**, *78*, 403.
31. Schwarz, H. A.; Dodson, R. W. *J. Phys. Chem.* **1989**, *93*, 409.
32. Surdhar, P. S.; Mezyk, S. P.; Armstrong, D. A. *J. Phys. Chem.* **1989**, *93*, 3360.
33. Hori, Y.; Suzuki, S. *Bull. Chem. Soc. Jpn.* **1982**, *55*, 660.
34. Aylmer-Kelly, A. W. B.; Bewick, A.; Cantrill, P. R.; Tuxford, A. M. *Faraday Discuss. Chem. Soc.* **1973**, *56*, 96.
35. Paik, W.; Andersen, T. N.; Eyring, H. *Electrochim. Acta* **1969**, *14*, 1217.
36. Buxton, G. V.; Sellers, R. M. *J. Chem. Soc., Faraday Trans. I* **1973**, *69*, 555.
37. Hori, Y.; Koga, O.; Yamazaki, H.; Matsuo, T. *Electrochim. Acta* **1995**, *40*, 2617.
38. Oda, I.; Ogasawara, H.; Ito, M. *Langmuir* **1996**, *12*, 1094.
39. Hori, Y.; Murata, A.; Takahashi, R.; Suzuki, S. *Chem. Commun.* **1988**, 17.
40. Watanabe, K.; Nagashima, U.; Hosoya, H. *Appl. Surf. Sci.* **1994**, *75*, 121.
41. Hori, Y.; Takahashi, I.; Koga, O.; Hoshi, N. *J. Mol. Catal. A: Chem.* **2003**, *199*, 39.
42. Takahashi, I.; Koga, O.; Hoshi, N.; Hori, Y. *J. Electroanal. Chem.* **2002**, *533*, 135.
43. Astruc, D. In *Transition-Metal Nanoparticles in Catalysis*; Astruc, D., Ed.; Wiley-VCH: Weinheim, Germany, 2007; Vol. 1, p 1.
44. Somorjai, G. A.; Tao, F.; Park, J. Y. *Top. Catal.* **2008**, *47*, 1.
45. Kim, J. J.; Summers, D. P.; Frese, K. W., Jr. *J. Electroanal. Chem.* **1988**, *245*, 223.
46. Koga, O.; Nakama, K.; Murata, A.; Hori, Y. *Denki Kagaku* **1989**, *57*, 1137.
47. Kyriacou, G.; Anagnostopoulos, A. *J. Electroanal. Chem.* **1992**, *322*, 233.
48. Frese, K. W., Jr. *J. Electrochem. Soc.* **1991**, *138*, 3338.
49. Yamamoto, T.; Tryk, D. A.; Fujishima, A.; Phata, H. *Electrochim. Acta* **2002**, *47*, 3327.

50. Sanchez-Sanchez, C. M.; Montiel, V.; Tryk, D. A.; Aldaz, A.; Fujishima, A. *Pure Appl. Chem.* **2001**, *12*, 1917.
51. Tryk, D. A.; Yamamoto, T.; Kokubun, M.; Hirota, K.; Hashimoto, K.; Okawa, M.; Fujishima, A. *Appl. Organomet. Chem.* **2001**, *15*, 113.
52. Yamamoto, M.; Tryk, D. A.; Hashimoto, K.; Fujishima, A.; Okawa, M. *J. Electrochem. Soc.* **2000**, *147*, 3393.
53. Yamamoto, T.; Hirota, K.; Tryk, D. A.; Hashimoto, K.; Fujishima, A.; Okawa, M. *Chem. Lett.* **1998**, 825.
54. Magdesieva, T. V.; Yamamoto, T.; Tryk, D. A.; Fujishima, A. *J. Electrochem. Soc.* **2002**, *149*, D89.
55. Dealacout, C.; Ridgway, P. L.; Kerr, J. B.; Newman, J. *J. Electrochem. Soc.* **2008**, *155*, 42.
56. DeWulf, D. W.; Bard, A. J. *Catal. Lett.* **1988**, *1*, 73.
57. Cook, R. L.; MacDuff, R. C.; Sammells, A. F. *J. Electrochem. Soc.* **1990**, *137*, 607.
58. Cook, R. L.; MacDuff, R. C.; Sammells, A. F. *J. Electrochem. Soc.* **1988**, *135*, 1470.
59. Cook, R. L.; MacDuff, R. C.; Sammells, A. F. *J. Electrochem. Soc.* **1990**, *137*, 187.
60. Hori, Y.; Konishi, H.; Futamura, T.; Murata, A.; Koga, O.; Sakurai, T.; Ohta, K *Electrochim. Acta* **2005**, *50*, 5354.
61. Komatsu, S.; Tanaka, M.; Okumura, A.; Kunugi, A. *Electrochim. Act.* **1995**, *40*, 745.
62. Hara, K.; Sakata, T. *Anal. Sci. Technol.* **1995**, *8*, 683.
63. Hara, K.; Sakata, T. *Bull. Chem. Soc. Jpn.* **1997**, *70*, 571.
64. Hori, Y.; Ito, H.; Okano, K.; Nagasu, K.; Sato, S. *Electrochim. Act.* **2003**, *48*, 2651.
65. Hori, Y.; Murata, A.; Ito, S.; Yoshinami, Y.; Koga, O. *Chem. Lett.* **1989**, 1567.
66. Shibata, M.; Yoshida, K.; Furuya, N. *J. Electrochem. Soc.* **1998**, *145*, 595.
67. Shibata, M.; Furuya, N. *J. Electroanal. Chem.* **2001**, *507*, 177.
68. Shibata, M.; Furuya, N. *Electrochim. Act.* **2003**, *48*, 3953.
69. Ikeda, S.; Ito, T.; Azuma, K.; Ito, K.; Noda, H. *Denki Kagaku* **1995**, *65*, 303.
70. Shibata, H.; Moulijn, J.; Mul, G. *Catal. Lett.* **2008**, *123*, 186.
71. Centi, G.; Perathoner, S. *ChemSusChem* **2010**, *3*, 195.
72. Doi, R.; Ichikawa, S.; Hida, H. Patent JP P08296077, 1995.
73. Ichikawa, S.; Doi, R. *Catal. Today* **1996**, *27*, 271.
74. Centi, G.; Perathoner, S. *Catal. Today* **2009**, *148*, 191.
75. Centi, G.; Perathoner, S. *Catal. Today* **2010**, *150*, 151.
76. Li, W.; Liang, C.; Qiu, J.; Zhou, W.; Han, H.; Wei, Z.; Sun, G.; Xin, Q. *Carbon* **2002**, *40*, 791–794.
77. Li, W.; Liang, C.; Zhou, W.; Qiu, J.; Zhou, Z.; Sun, G.; Xin, Q. *J. Phys. Chem. B* **2003**, *107*, 6292–6299.
78. Li, W.; Wang, X.; Chen, Z.; Waje, M.; Yan, Y. *J. Phys. Chem. B* **2006**, *110*, 15353–15358.
79. Wang, X.; Li, W.; Chen, Z.; Waje, M.; Yan, Y. *J. Power Sources* **2006**, *158*, 154–159.

80. Pan, X.; Fan, Z.; Chen, W.; Ding, Y.; Luo, H.; Bao, X. *Nat. Mater.* **2008**, *6*, 507.
81. Pan, X.; Bao, X. *Chem. Commun.* **2008**, 6271.